External Barium Block of *Shaker* Potassium Channels: Evidence for Two Binding Sites

R. S. HURST,* R. LATORRE,‡ L. TORO,* and E. STEFANI*

From the *Department of Anesthesiology, University of California at Los Angeles, Los Angeles, California 90095; and the ‡University of Chile and Centro de Estudios Cientificos de Santiago, Santiago, Chile

ABSTRACT External barium ions inhibit K^+ currents of *Xenopus* oocytes expressing *Sh*H4 Δ6-46, the non-inactivating deletion of the *Shaker* K^+ channel. At the macroscopic level, Ba^{2+} block comprises both a fast and a slow component. The fast component is less sensitive to Ba^{2+} (apparent dissociation constant at 0 mV, $K_{(0)}$, ≈ 19.1 mM) than the slow component and is also less voltage dependent (apparent electrical distance, δ, ≈ 0.14). The slow component ($K_{(0)}$, ≈ 9.4 mM, δ ≈ 0.25) is relieved by outward K^+ current, which suggests that the corresponding binding site resides within the channel conduction pathway. At the single channel level, the fast component of block is evidenced as an apparent reduction in amplitude, suggesting an extremely rapid blocking and unblocking reaction. In contrast, the slow component appears to be associated with long blocked times that are present from the beginning of a depolarizing command. Installation of the slow component is much slower than a diffusion limited process; for example, the blocking time constant (τ) produced by 2 mM Ba^{2+} is ~159 s (holding potential, HP = −90 mV). However, the blocking rate of this slow component is not a linear function of external Ba^{2+} and tends to saturate at higher concentrations. This is inconsistent with a simple bi-molecular blocking reaction. These features of external Ba^{2+} block can be accounted for by a simple model of two sequential Ba^{2+} binding sites, where the deeper of the two sites produces the slow component of block.

INTRODUCTION

Barium ions are only slightly larger in crystal radius than K^+, yet they can block the pore of many voltage-gated K^+ channels (e.g., Armstrong and Taylor, 1980; Eaton and Brodwick, 1980; Grissmer and Cahalan, 1989; Wollmuth, 1994). When applied to the internal side of the squid axon-delayed rectifier, Ba^{2+} binds at a site that is accesible only when the channel is open, well within the membrane field (Armstrong and Taylor, 1980; Eaton and Brodwick, 1980). Molecular biological approaches using cloned voltage-gated K^+ channels are providing insight to the structural deter-

Address correspondence to Raymond S. Hurst, Department of Anesthesiology, BH-612 CHS, University of California at Los Angeles, Los Angeles, CA 90095-1778.

J. GEN. PHYSIOL. © The Rockefeller University Press · 0022-1295/95/12/1087/19 $2.00
Volume 106 December 1995 1069–1087

minants governing internal Ba^{2+} block. For example, a single amino acid substitution within the putative pore-forming region of DRK1, a cloned delayed rectifier, was shown to decrease the dissociation rate of internal Ba^{2+} by more than 10 times (Taglialatela, Drewe, and Brown, 1993). Similarly, the sixth putative membrane-spanning region (S6) and two positions within the S4-S5 loop have been demonstrated to contribute to internal Ba^{2+} block of the *Shaker* K^+ channel (Slesinger, Jan, and Jan, 1993; Lopez, Jan, and Jan, 1994).

Barium ions can also block voltage-gated K^+ channels when applied to the extracellular side of the membrane (Armstrong and Taylor, 1980; Armstrong, Swenson, and Taylor, 1982; Grissmer and Cahalan, 1989; Wollmuth, 1994). Unlike internal block, external Ba^{2+} block of the squid axon-delayed rectifier does not require channel opening, even though the binding site resides within the K^+ conduction pathway (Armstrong and Taylor, 1980; Armstrong et al., 1982). In contrast, external Ba^{2+} blocks the T-lymphocyte voltage-dependent K^+ channel only after the channel has opened (Grissmer and Cahalan, 1989). The effect of extracellular Ba^{2+} on the M-like voltage-dependent K^+ current of rod photoreceptors is more complicated. In this case, Ba^{2+} alters the voltage sensitivity and kinetics of the channel as well as reducing the conductance (Wollmuth, 1994).

The present work extends the study of external Ba^{2+} block to the cloned *Shaker* K^+ channel. It provides evidence that the *Shaker* channel has at least two external Ba^{2+} blocking sites. One is a relatively low affinity site with an apparent dissociation constant at 0 mV($K_{(0)}$) of ~19.1 mM. This site gives rise to a quasi-instantaneous component of block in macroscopic currents. The voltage dependence of this fast component suggests that the binding site resides ~14% of the way across the membrane electric field. The second blocking site is more sensitive to Ba^{2+} ($K_{(0)} \approx 9.4$ mM) and is associated with a very slow component of block. This site resides ~25% of the way across the membrane electric field, within the ion conducting pathway. Unlike the expected results for a bimolecular reaction, the blocking rate of this slow component tends to saturate at higher concentrations of Ba^{2+}. These features of block can be accounted for by a model composed of two sequential Ba^{2+} blocking sites. In this model, the second and more internal site is associated with the slow component of block.

METHODS

The deletion construct of *Shaker*, *Sh*H4 D6-46, was used in this study to prevent complications of fast or N-type inactivation (Hoshi, Zagotta, and Aldrich, 1990). *Sh*H4 Δ6-46 (*Sh*H4-IR for inactivation removed) encoding RNA was synthesized in vitro using T7 RNA polymerase and unmethylated CAP analogue (Pharmacia, Piscataway, NJ), according to published methods (Stefani, Toro, Perozo, and Bezanilla, 1994). Collagenase (200 U/ml; Gibco Laboratories, Grand Island, NY) treated *Xenopus* oocytes (stage V–VI) were injected with ~5 ng of RNA in 50 nl of water. Oocytes were maintained at 18°C in an amphibian saline solution supplemented with gentamycin (50 μg/ml). Voltage-clamp recordings were performed at room temperature 2–5 d after injection.

Electrophysiology

Macroscopic ionic and gating currents were recorded using the cut-open oocyte vaseline gap (COVG) voltage-clamp technique (Taglialatela, Toro, and Stefani, 1992; Stefani et al., 1994). The

extracellular solution was perfused manually, requiring ~5 s for complete exchange. Intracellular perfusion (5 ml/h) was made through a small quartz cannula ~50 μm in diameter inserted into the bottom of the oocyte. Linear leak and capacity components were compensated analogically and subtracted on line using the P/4 method from a subtracting holding potential of −90 mV for ionic current and −120 mV for gating current. All experiments were filtered at one-fifth the sampling frequency.

Single-channel cell-attached patch clamp experiments were performed on oocytes after manual removal of the vitelline membrane. Test pulses to 30 mV for 100 ms were given once per second. Data was digitized at 50 or 100 μs/point after low-pass filtering at 2 kHz. Single-channel records were corrected off line for linear leak and capacity currents using customized software. Open and closed transitions were detected by the half amplitude threshold criterion using the TRANSIT software (A. M. J. VanDongen, Duke University, Chapel Hill, NC).

Solutions

Solutions were made by mixing stock isotonic solutions (240 mOsm) of the main cation containing 10 mM *N*-[2-hydroxyethyl]piperazine-*N'*-[2-ethanesulfonic acid] (HEPES) at pH 7.0. The external solution in experiments using the COVG was 115 mM sodium methanesulphonate (NaMES), 2 mM calcium methanesulphonate [$Ca(MES)_2$], 2 mM potassium methanesulphonate (KMES), 0.1 mM EGTA, and 10 mM HEPES. In barium experiments, isotonic barium methanesulphonate [$Ba(MES)_2$] replaced NaMES in the following solution: 117 mM NaMES, 2 mM KMES, and 10 mM HEPES. The solution in contact with the intracellular compartment was 120 mM potassium glutamate (KGLU) buffered with 10 mM HEPES, except for internal perfusion experiments. In those experiments, the intracellular solution was perfused with 100 mM *n*-methyl-D-glucamine methanesulphonate (NMG-MES), 10 mM KMES, and 10 mM HEPES. The intracellular microelectrode was filled with 2.7 M NaMES, 10 mM NaCl, 10 mM EGTA, and 10 mM HEPES. In the cell-attached patch clamp experiments, a depolarizing bath solution was used containing 117 mM KMES, 2 mM $MgCl_2$, 0.1 mM EGTA, and 10 mM HEPES. The control pipette solution was 117 mM NaMES, 2 mM KCl, and 10 mM HEPES; in the barium experiments, isotonic $Ba(MES)_2$ replaced NaMES in the following: 118 mM NaMES, 2 mM KCl, 10 mM HEPES.

Data Analysis

All data are reported as mean ± SD unless otherwise stated; in macroscopic recordings, n = number of oocytes; in single-channel recordings, n = number of patches. Macroscopic Ba^{2+} dose-response measurements were performed by perfusing the extracellular solution in the cut-open oocyte configuration; Ba^{2+} was washed out between each application. The current amplitude was determined at the end of an 8-ms depolarizing command to 30 mV repeated once every 5 s. The peak current amplitude (I) of sequential pulses was fitted to a single exponential term

$$I = A\exp(-t/\tau) + C \quad (1)$$

to derive the initial and steady state (C) levels of the slow blocking component (see Fig. 2 *A*). The fast blocking component was taken as the difference between the current amplitude in the absence of Ba^{2+} and the initial value of the slow component. Barium inhibition data for the individual components were fit by least squares minimization to

$$K = 100 \cdot [Ba]^n / ([Ba]^n + K^n), \quad (2)$$

where K is the apparent dissociation constant and n is the Hill coefficient.

The dependence of slow component on holding potential was determined by measuring the apparent dissociation constant at holding potentials of −70, −90, and −120 mV; in each case, the

membrane was depolarized to 30 mV for 8 ms repeated once every 5 s. The apparent dissociation constant was plotted against the holding potential and fit to the Woodhull model

$$K_{(V)} = K_{(0)} \exp(-z\delta VF/RT), \quad (3)$$

where $K_{(V)}$ is the apparent dissociation constant, $K_{(0)}$ is the apparent dissociation constant at 0 mV, z is the valence on the blocking ion, δ is the fraction of the electric field, V is the membrane potential, and F, R, and T have their usual meaning (Woodhull, 1973).

The voltage dependence of the fast component was assayed by measuring the instantaneous current–voltage (I–V) relation in 80 mM external K^+. The instantaneous block produced by 20 mM Ba^{2+} was compared at potentials between −100 and 25 mV in 5-mV increments. The I–V relation measured in the presence of Ba^{2+} was fit to

$$I = \frac{I_o}{1 + \dfrac{[Ba^{2+}]}{K_{(0)} \exp(-z\delta VF/RT)}}, \quad (4)$$

where I is the current amplitude and I_o is the control amplitude measured in the absence of Ba^{2+}.

Competition between external Ba^{2+} and K^+ was tested by measuring the blocking potency of 20 mM Ba^{2+} at different concentrations of external K^+. The reciprocal of the probability of block ($1/P_{blk}$), assayed by an 8-ms pulse to 30 mV repeated every 5 s, was plotted against external K^+ concentration. These data were fit to

$$1/P_{blk} = 1 + K_{Ba}\left(1 + \frac{[K^+]}{K_K}\right)\left(\frac{1}{[Ba^{2+}]}\right), \quad (5)$$

where K_{Ba} is the dissociation constant of Ba^{2+} and K_K is the dissociation constant of K^+ (Gaddum, 1936; Vergara and Latorre, 1983).

RESULTS

External Ba^{2+} Block of Sh*H4-IR*

External Ba^{2+} inhibits the outward K^+ current in oocytes expressing the noninactivating deletion of the *Shaker* potassium channel, *Sh*H4-IR (*Sh*H4 Δ6-46; Hoshi et al., 1990). Current inhibition by Ba^{2+} is strongly time dependent, as illustrated in Fig. 1 *A*. These traces are shown at 20-s intervals (pulses were given once every 5 s) immediately before and after the addition of 2 mM Ba^{2+} to the external solution. Outward currents decayed to their new steady state level after ~7 min, giving a time constant of block (τ) by 2 mM Ba^{2+} of 159 ± 31 s (n = 4, HP = −90 mV). Fig. 1 *B* demonstrates that this blocking event is not "use dependent" and can occur when the channel is closed. In this experiment, 2 mM Ba^{2+} was added to the external solution while holding the channels closed at −90 mV. After 5–7 min in these conditions, a single depolarizing command to 30 mV was given to assay the level of block. The outward current evoked by the test pulse was substantially reduced (50.8% ± 7.4%, n = 3) from the beginning of the pulse, even though the channels were never previously opened in the presence of Ba^{2+}. This provides strong evidence that Ba^{2+} can block *Sh*H4-IR while the channel is in the closed conformation, consistent with the well-established idea that the channel gate is on the cytoplasmic

side of the membrane (Armstrong, 1966, 1969, 1971; Armstrong and Taylor, 1980; Armstrong et al., 1982).

Ba^{2+} Block Comprises a Fast and Slow Component

Installation of the closed-blocked state by Ba^{2+} was assayed with a brief (8 ms) test pulse to 30 mV repeated once every 5 s (Fig. 2 *A*). Adding Ba^{2+} externally (Fig. 2 *A*, 20 mM) revealed two components of block, a quasi instantaneous component followed by a slower exponentially decaying phase. To quantify these two components, the slow current decay produced by external Ba^{2+} was fit to a single exponential term (*continuous line*). Extrapolating the fit to times zero and infinity provided estimates of the initial and steady state levels of this slow component, respectively. The fast component was simply taken as the difference between the current amplitude in the absence of Ba^{2+} and the initial amplitude of the slow component. In this way the fast and slow components could be analyzed separately, generating the individual dose-response relationships shown in Fig. 2 *B*. Due to the extremely slow blocking and unblocking kinetics, the 8-ms test pulse should have little effect on the slow component of block. Therefore, the dose-response relationship of this slow component largely reflects the affinity of closed channels for Ba^{2+}. In contrast, the fast component re-equilibrates much faster than the test pulse, as evidenced in single-channel experiments, and therefore reflects the Ba^{2+} affinity of open channels (see below). Interestingly, the relaxation of the current amplitude following the washout of 20 mM Ba^{2+} was composed of only one component (Fig. 2 *A*). This suggests that a single rate limiting process controls the recovery from Ba^{2+} block (see Discussion).

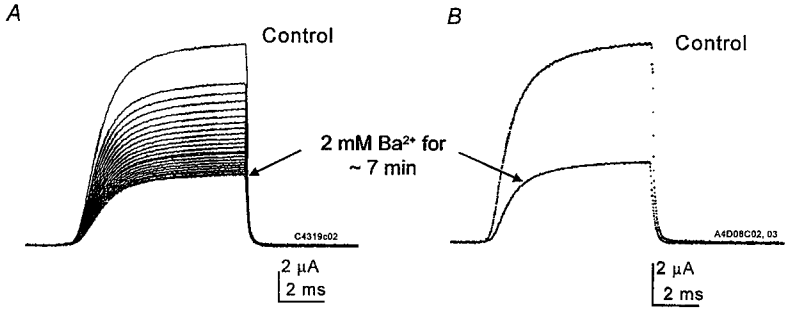

FIGURE 1. External Ba^{2+} can block the closed state of *Sh*H4-IR. (*A*) A depolarizing command to 30 mV was given under control conditions (*upper trace*) and at 5-s intervals after the addition of 2 mM Ba^{2+} to the external solution; every fourth trace is shown. The total time of the experiment was ~7 min. (*B*) The upper trace was recorded under control conditions, and the lower was recorded approximately 7 min after the addition of 2 mM Ba^{2+} to the external solution. In this case, Ba^{2+} was added to the external solution while holding the membrane at −90 mV; this holding potential was maintained for the entire duration between the two pulses shown.

Consistent with the idea that the slow component reflects Ba^{2+} block of closed channels, this component was influenced by the holding potential (Fig. 3 *A*). That

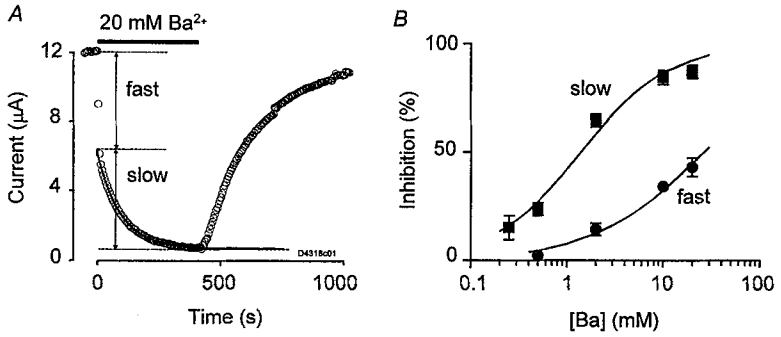

FIGURE 2. External Ba^{2+} block block of *Sh*H4-IR comprises a fast and slow component. (*A*) Time course of the installation and relief of block by 20 mM Ba^{2+} assayed by an 8-ms command pulse to 30 mV repeated once every 5 s. Symbols show the current evoked at the end of each successive pulse. The decaying phase was fitted with a single exponential term (*continuous line*) to quantify each component (see Methods). (*B*) Ba^{2+} inhibition curves for the fast and slow components of block. Symbols show the mean ± SD of three to six oocytes; when not shown, the error is less than the size of the symbol. The apparent dissociation constant (K) and Hill coefficient (n) were as follows: for the fast component, $K = 26.6 \pm 7.4$ mM, $n = 0.8 \pm 0.03$ (mean ± SD, $n = 3$); for the slow component, $K = 1.3 \pm 0.1$ mM, $n = 1.0 \pm 0.1$ (mean ± SD, $n = 3$).

is, the slow component became more pronounced when the holding potential was hyperpolarized from −70 to −120 mV, even though the test pulse was always given to 30 mV. This can only be explained if Ba^{2+} interacts with channels at the holding potential, during which time the channels should be closed. According to the

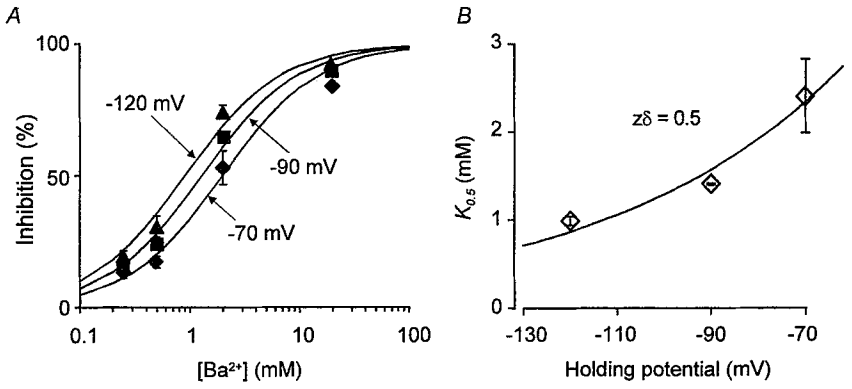

FIGURE 3. The slow component of external Ba^{2+} block is dependent on holding potential. (*A*) Ba^{2+} concentration response curves for the slow component measured at holding potentials of −70, −90, and −120 mV. Currents were evoked by an 8-ms test pulse to 30 mV repeated once every 5 s. Symbols are the mean inhibition, in percent (± SEM), of three to six oocytes; when not shown, the error bars are less than the size of the symbol. The following are the apparent dissociation constants (K) ± SEM for the slow component as a function of holding potential: for −70 mV, $K = 2.4 \pm 0.4$ mM, $n = 3$; for −90 mV, $K = 1.4 \pm 0.1$ mM, $n = 4$; for −120 mV, $K = 1.0 \pm 0.1$ mM, $n = 3$. (*B*) Apparent dissociation constants from *A* as a function of holding potential. Symbols are the mean ± SEM of three to four oocytes. The solid line is the least squares fit to the Woodhull function (Eq. 3), $z\delta = 0.5$ and $K_0 = 9.4$ mM.

Woodhull model, the influence of holding potential on the slow component suggests that barium crosses ~25% of the membrane electric field to produce the slow component of block (Fig. 3 *B*; Woodhull, 1973).

Relief of Block by K^+

Prolonged depolarizations in the presence of Ba^{2+} reveal a pronounced rising phase or hump in the current trace (Fig. 4 *A*). For example, 2 mM Ba^{2+} reduced

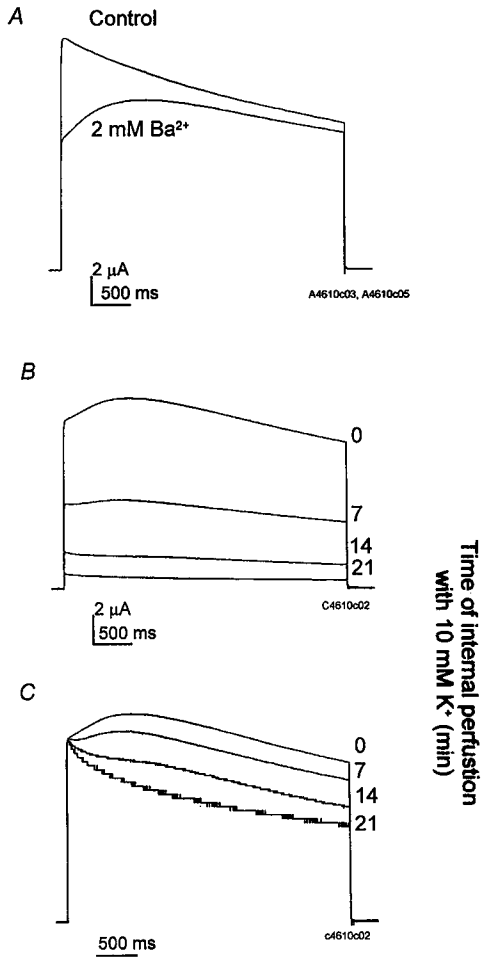

FIGURE 4. Outward K^+ current relieves Ba^{2+} block. (*A*) K^+ current evoked by a 3.6-s depolarizing command to 30 mV in the presence (*lower trace*) and absence (*upper trace*) of 2 mM external Ba^{2+}. (*B* and *C*) Currents evoked in the presence of 2 mM Ba^{2+} at different times after the start of internal perfusion with low (10 mM) K^+. The number to the right of each trace indicates the time in minutes in which the internal oocyte compartment was perfused (50 ml/h). In *C*, the same traces as *B* normalized to the initial current amplitude upon depolarization, which was as follows; for 0 min, 11.7 µA; for 7 min, 5.8 µA; for 14 min, 2.4 µA; and for 21 min, 0.9 µA.

the current shown in Fig. 4 *A* by 44.6% at the beginning and only 8.9% at the end of a 3.6-s depolarizing command. Given that the fast component can only account for a 14.4% ± 2.7% (n = 4) reduction in current at this concentration, this rising phase primarily reflects the relief of the slow component of block. Two possible mechanisms can account for this relief of Ba^{2+} block—an intrinsic voltage dependence of block and/or K^+ flow through the channel. The latter is equivalent to the "knock-off" effect that has long been described for the interaction between per-

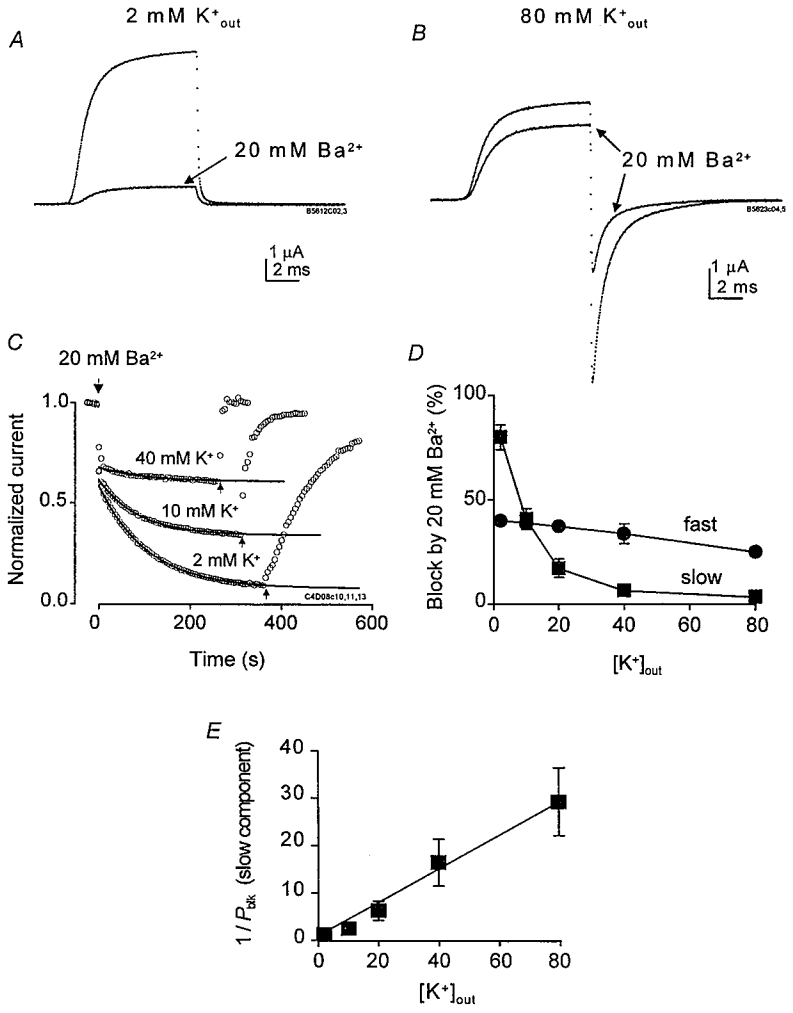

FIGURE 5. External K^+ relieves Ba^{2+} block. (*A* and *B*) Currents evoked at 30 mV in control conditions and at quasi-steady state block by 20 mM external Ba^{2+}. The external solution contained either 2 mM K^+ (*A*) or 80 mM K^+ (*B*). (*C*) Time course of block by 20 mM Ba^{2+} in three concentrations of extracellular K^+. Symbols show the normalized current at the end of an 8-ms pulse to 30 mV repeated once every 5 s. Ba^{2+} was added at time zero, and the arrow indicates the time of wash. The continuous line shows the least squares fit of the decaying phase to a single exponential term. (*D*) Block, in percent, for the fast component (*solid circles*) and slow component (*solid squares*) produced by 20 mM Ba^{2+} as a function of extracellular K^+ concentration. Data are the mean ± SD of four or five oocytes. (*E*) Same data as in *D* for the slow component plotted as the reciprocal of the probability of block ($1/P_{blk}$). The continuous line is the fit to a model of competitive inhibition of Ba^{2+} block by extracellular K^+ (Eq. 5; Gaddum, 1936; Vergara and Latorre, 1983).

meant ions and channel blockers (for example, Armstrong, 1971; Bezanilla and Armstrong, 1972; Adelman and French, 1978). To distinguish between these two possibilities, we measured the relief of Ba^{2+} block, as indicated by the outward hump, at different concentrations of intracellular K^+. Fig. 4 *B* shows that lowering the internal K^+ concentration reduces both the outward K^+ current and the relief of Ba^{2+} block. This is more evident in Fig. 4 *C* showing the same traces scaled to their initial amplitude; the outward hump is clearly diminished at longer times of internal perfusion. This dependence on internal K^+ for the relief of Ba^{2+} block provides strong evidence that the site associated with the slow component resides in the K^+ conduction pathway (Armstrong, 1971).

Previous studies have shown that extracellular K^+ can also reduce Ba^{2+} block of voltage-dependent K^+ currents (Århem, 1980; Armstrong and Taylor, 1980; Wollmuth, 1994). Similarly, extracellular K^+ decreased external Ba^{2+} block of *Sh*H4-IR (Fig. 5, *A* and *B*). This resulted primarily from a marked reduction in the slow component of block (Fig. 5, *C* and *D*). For example, the fast block produced by 20 mM

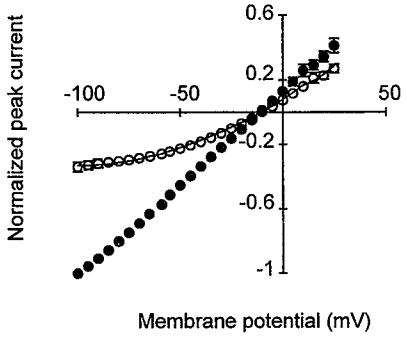

FIGURE 6. Instantaneous current-voltage relationship measured in 80 mM external K^+. The instantaneous current–voltage (*I–V*) relationship was measured in 80 mM external K^+ by depolarizing the membrane to 40 mV and then stepping to potentials between −100 and 25 mV in 5-mV increments. The peak amplitude of the tail current is plotted as a function of the test potential in the absence (*solid circles*) and in the presence of 20 mM external Ba^{2+} (*open circles*). These data were fitted to a voltage-dependent blocking model to obtain an apparent electrical distance (δ) for the fast component of block (*continuous curve*, Eq. 4). This fit gave a value for δ of 0.14 ± 0.02. Data are the mean ± SD of five oocytes; when not shown, the error bar is smaller than the size of the symbol.

Ba^{2+} was reduced from 40.0% ± 2.5% (n = 5) to 33.7% ± 4.5% (n = 4) by increasing the extracellular K^+ from 2 mM to 40 mM. In contrast, the slow component produced by 20 mM Ba^{2+} was reduced from 80.1% ± 5.9% (n = 5) to only 6.6% ± 1.9% (n = 4) when external K^+ was raised from 2 mM to 40 mM. Fig. 5 *E* shows that the relationship between the slow component and extracellular K^+ is well described by a model of competitive inhibition (Eq. 5; Gaddum, 1936; Vergara and Latorre, 1983). According to this model, the apparent dissociation constant for K^+ is 0.20 ± 0.04 mM (n = 4). This result suggests that the binding site associated with the slow component of block overlaps with a K^+ binding site (Århem, 1980; Vergara and Latorre, 1983; Grissmer and Cahalan, 1989).

Because high extracellular K^+ can markedly reduce the slow component of block (Fig. 5), these conditions were used to isolate the fast component and determine its voltage dependence. Fig. 6 shows the instantaneous current–voltage (*I–V*) relationship measured in 80 mM external K^+. In this experiment, the membrane was depolarized to 40 mV and then repolarized to a series of test potentials between −100

and 25 mV. The peak of the tail current is plotted against the test potential in the absence (*solid circles*) and presence of 20 mM Ba^{2+} (*open circles*). This current is proportional to the number of channels open at the end of the depolarizing command and the channel conductance at the test potential (e.g., Stefani et al., 1994). Therefore, the nonlinearity in the presence of Ba^{2+} reflects a decreased conductance at

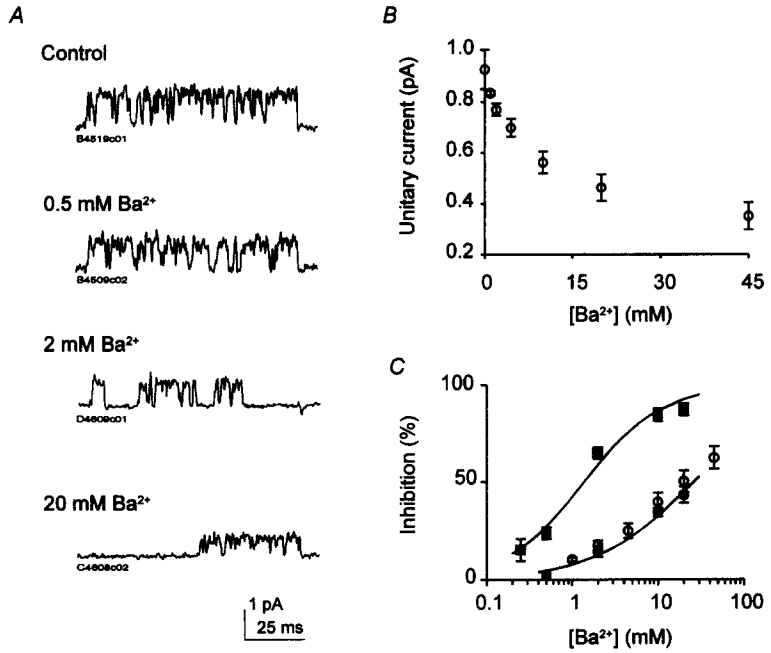

FIGURE 7. Ba^{2+} reduces the apparent single-channel amplitude. Cell-attached patch-clamp recordings with different concentrations of Ba^{2+} in the pipette. (*A*) Single-channel records from four different patches with the indicated concentration of Ba^{2+} in the pipette; data filtered at 1 kHz. In each case the membrane was held at −90 mV and step depolarized to 30 mV for 100 ms, repeated once every 1 s. (*B*) Plot of the unitary amplitude as a function of Ba^{2+} concentration. Data are the mean ± SD of three to eight patches. (*C*) Unitary current amplitudes from *B* converted to a percentage reduction as a function of Ba^{2+} concentration (*open circles*). Inhibition values were based on a control amplitude of 0.93 pA. Also plotted are the data and fits of the dose-response relationships for the slow component (*solid squares*) and fast component (*solid circles*) of the macroscopic currents (same data as in Fig. 2 *B*).

hyperpolarized potentials. The continuous curve in Fig. 6 shows the fit of this data to a voltage-dependent blocking model (Eq. 4). This fit suggests that Ba^{2+} crosses 14% ± 2% ($n = 5$) of the membrane electric field to produce the fast component of block.

Ba^{2+} Block of Single Sh*H4-IR Channels*

External Ba^{2+} had two major effects on single *Sh*H4-IR channels recorded in the cell-attached patch-clamp configuration. One effect was to reduce the apparent sin-

gle-channel amplitude (Fig. 7, *A* and *B*). For example, the mean current amplitude at 30 mV in the absence of Ba^{2+} was 0.93 ± 0.08 pA (n = 3) as compared with only 0.46 ± 0.05 pA (n = 5) with 20 mM Ba^{2+} in the pipette. This effect of Ba^{2+} on the apparent unitary amplitude was dose dependent and had a concentration response relationship very similar to the fast component of block in macroscopic currents (Fig. 7, *B* and *C*). The apparent reduction in amplitude most likely results from an

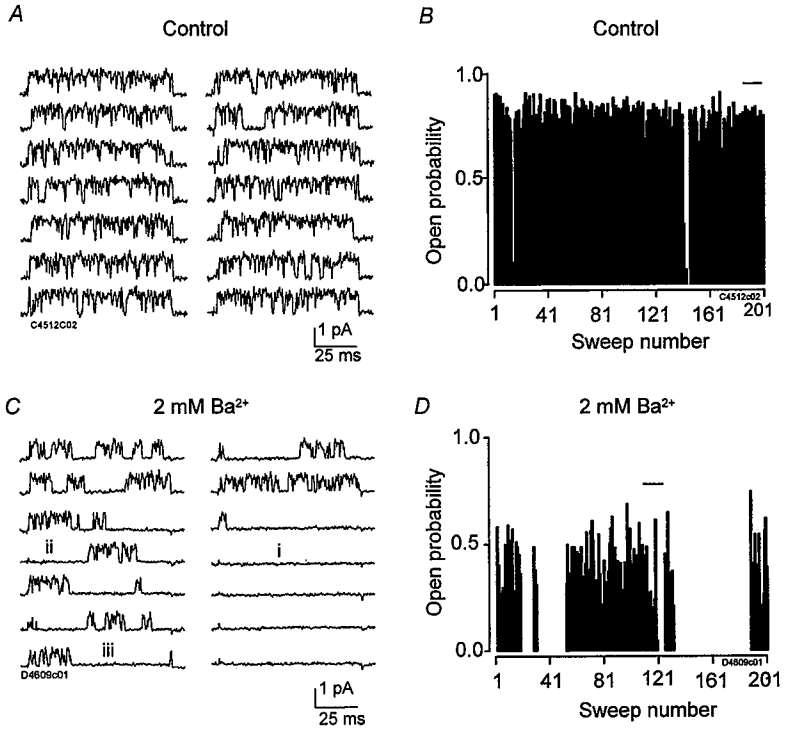

FIGURE 8. Ba^{2+} introduces discrete blocked times in single-channel records. (*A* and *C*) Consecutive sweeps recorded in control conditions (*A*) and with 2.0 mM Ba^{2+} in the pipette (*C*). The membrane was held at −90 mV and stepped to 30 mV for 100 ms, repeated once every 1 s; data are filtered at 1 kHz. In *C*, the lowercase roman numerals indicate three subtypes of discrete blocking events: (i) no openings, (ii) blocked times that precede channel opening, and (iii) blocked times that follow channel opening. (*B* and *D*) Plots of open probability versus sweep number for 200 consecutive sweeps in control conditions (*B*) and with 2.0 mM Ba^{2+} in the pipette (*D*). The horizontal bars in *B* and *D* indicate the sweeps shown in *A* and *C*, respectively.

extremely rapid blocking and unblocking event that exceeds the temporal resolution of these experiments (Woodhull, 1973; Coronado and Miller, 1979; Horn, Patlak, and Stevens, 1981; Yellen, 1984).

A second effect of Ba^{2+} at the single-channel level was to reduce the channel open probability by introducing discrete blocking events. These blocked times can be separated into three subtypes: (i) null sweeps or sweeps without channel open-

ing; (ii) blocked times that precede channel opening; and (iii) blocked times that follow channel opening (Fig. 8 *C*). Blocking events that follow channel opening represent Ba^{2+} block of open channels or channels very near the open state. In contrast, both the null sweeps and the sweeps that are blocked at the beginning of the depolarizing pulse most likely reflect channels that were blocked prior to opening, i.e., a closed-blocked channel. Fig. 8, *B* and *C*, shows that the null sweeps in the presence of external Ba^{2+} often appear in clusters that can last for several tens of sweeps (100-ms command pulses to 30 mV repeated once per second; HP = −90 mV). This suggests that the underlying closed-blocked event is relatively long-lived.

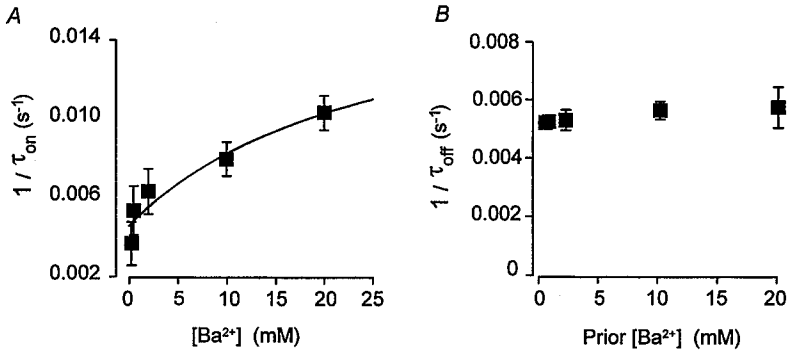

FIGURE 9. Blocking and recovery time course of the slow component. (*A*) The reciprocal of the blocking time constant ($1/\tau_{on}$) of the slow component is plotted as a function of external Ba^{2+} concentration; τ_{on} was obtained by fitting the current decay in the presence of external Ba^{2+} to a single exponential term (see Fig. 2 *A*). Symbols are the mean ± SD of three to five oocytes; the continuous line is the fit to a sequential two-site binding model (Eq. 6). (*B*) The reciprocal of the recovery rate ($1/\tau_{off}$) as a function of the prior blocking concentration of Ba^{2+}; in each case the wash solution was nominally free of Ba^{2+}. τ_{off} was obtained by fitting a single exponential to the relaxation phase following wash-out of the indicated concentration of Ba^{2+}. Symbols are the mean ± SD of three to five oocytes, except 0.25 mM, $n = 1$. The mean unblocking rate ($1/\tau_{off}$) from all concentrations was 0.0055 ± 0.0004 s^{-1}, $n = 16$.

DISCUSSION

External Ba^{2+} Blocks Sh*H4-IR at Two Distinct Sites*

The existence of two external Ba^{2+} blocking sites on *Sh*H4-IR was first suggested by the bi-phasic time course of block. It can be argued, however, that the fast component resulted from a nonspecific effect of charge screening (Imoto, Methfessel, Sakmann, Mishina, Mori, Konno, Fukuda, Kurasaki, Bujo, Fujita, and Numa, 1986; Kell and DeFelice, 1988; MacKinnon, Latorre, and Miller, 1989). In this case, the amplitude of the fast component should be dependent on the change in divalent ion concentration. In contrast, the fast component of block produced by 20 mM Ba^{2+} was not different when compared with control solutions containing either 2 mM Ca^{2+} (43.2% ± 4.3% block, $n = 5$) or 20 mM Ca^{2+} (40.9% ± 5.5% block, $n = 5$). In

other words, this fast component does not result simply from changing the divalent ion concentration. This provides evidence that a specific binding site controls the fast component of block.

In further support for the existence of two external Ba^{2+} binding sites, the blocking rate of the slow component ($1/\tau_{on}$) tends to saturate at high concentrations of Ba^{2+} (Fig. 9 *A*). In contrast, for a simple bimolecular reaction, the blocking rate is expected to increase linearly with blocker concentration. There are two possible mechanisms that can account for the observed saturation in the blocking rate. One is that external Ba^{2+} block could reflect a gross conformational change in the channel structure that closes the pore. In this case, the limiting blocking rate would reflect the rate limiting conformational change that closes the pore, not Ba^{2+} bind-

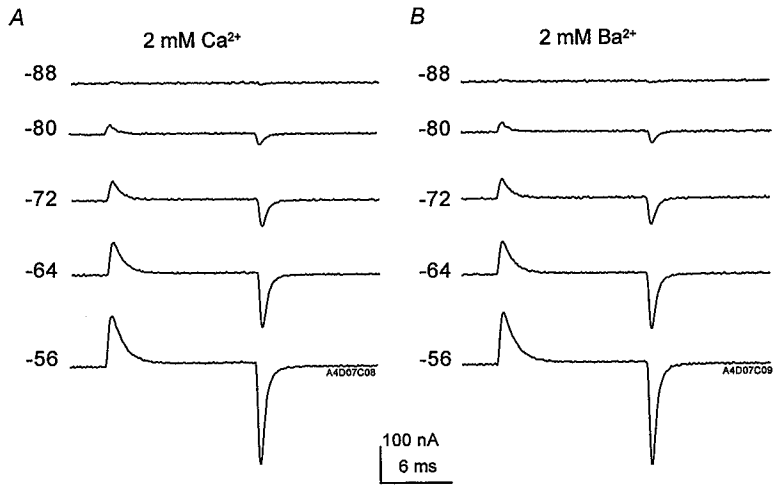

FIGURE 10. Ba^{2+} does not alter the gating charge movement at potentials hyperpolarized to channel opening. Gating currents recorded (*A*) before and (*B*) after ~6 min of exposure to 2 mM external Ba^{2+}. Currents were recorded at the indicated test potential; the holding potential was −90 mV and negative subtracting pulses of 1/4 of the test pulse ($P/-4$) were from −120 mV. Traces are the average of three sweeps.

ing. This possibility was investigated by measuring gating charge movement or "gating current." Because gating current is generated by protein rearrangements, it reflects the entire population of channels, not just those that conduct (for review, see Almers, 1978). Therefore, any significant change in the channel conformation induced by Ba^{2+} should be revealed by a change in the gating charge movement (McCormack, Joiner, and Heinemann, 1994; Taglialatela, Kirsch, VanDongen, Drewe, Hartmann, Joho, Stefani, and Brown, 1992). Fig. 10 shows that 2 mM Ba^{2+} did not notably alter the voltage dependence, kinetics, or quantity of gating charge movement at potentials hyperpolarized to channel opening. This argues that Ba^{2+} does not induce gross changes in the channel conformation. However, these experiments do not address the possibility that Ba^{2+} influences the final transition from

the closed to open state, which is thought to move relatively little charge (e.g., Zagotta and Aldrich, 1990; Koren, Liman, Logothetis, Nadal-Ginard, and Hess, 1990; Bezanilla, Perozo, and Stefani, 1994). This final charge movement is obscured in these experiments by the ionic current evoked at potentials that open the channel pore.

A second possible explanation for the saturation in blocking rate is that the slow component results from the binding of Ba^{2+} at the second of two sequential sites. This is illustrated in the following kinetic reaction scheme:

$$Ba^{2+} + Site1 - Site2 \underset{k_{off}(1)}{\overset{k_{on}(1)}{\rightleftharpoons}} Ba^{2+}:Site1 - Site2 \underset{k_{off}(2)}{\overset{k_{on}(2)}{\rightleftharpoons}} Site1 - Site2:Ba^{2+},$$

where Site 1 and Site 2 are two Ba^{2+} binding sites, Site 2 produces the slow component of block, and k_{on} and k_{off} are the respective binding and unbinding rates at Site 1 and Site 2. In this case, the blocking rate at Site 2 (slow component) will not depend on the bulk Ba^{2+} concentration, but instead will depend on the probability that Site 1 is occupied by Ba^{2+}. This blocking rate ($1/\tau_{on}$) is given by

$$1/\tau_{on} = k_{on}(2) \cdot ([Ba]/[Ba] + K_1) + k_{off}(2), \quad (6)$$

where K_1 is the dissociation constant of Site 1 and the ratio ($[Ba]/[Ba] + K_1$) is the probability that Site 1 is occupied by Ba^{2+}. This model can reasonably predict the observed saturation of the slow component blocking rate (continuous line in Fig. 9 *A*). In addition, it provides an independent estimate of the dissociation constant for the fast component (K_1 = 23.3 mM) and the unblocking rate of the slow component ($k_{off}(2) = 1/\tau_{off} = 0.0048\ s^{-1}$), both of which are in good agreement with the experimental results (see Figs. 2 *B* and 9 *B*, respectively). Consistent with the idea of two blocking sites, a mutation in the outer pore of *Sh*H4-IR [*Sh*H4-IR (T449Y)] can markedly reduce the slow blocking component without significantly altering the fast component (Hurst, Toro, and Stefani, 1995).

Ba^{2+} Block at the Single-channel Level and Its Relationship to the Macroscopic Current

Externally applied Ba^{2+} both reduced the apparent unitary amplitude and introduced discrete blocked times in single-channel records. Two lines of evidence suggest that the apparent reduction in channel amplitude induced by external Ba^{2+} corresponds to the fast component of block observed in macroscopic currents. First, both of these processes represent fast binding reactions. Given the low binding energy of the macroscopic fast component, $\Delta G = RT\ln K_1$ or −8.9 kJ/mol, the mean residency time giving rise to this component can be extremely short, approaching 3.7×10^{-7} s (see Hille, 1992). Blocking events of this duration would have been too fast to be resolved at the filtering frequency used in the single-channel experiments, and these events would simply appear as a reduction in the single-channel amplitude (Woodhull, 1973; Coronado and Miller, 1979; Horn et al., 1981; Yellen, 1984). Second, the apparent reduction in unitary amplitude has a dose-response relationship very similar to that of the fast component of block in

macroscopic currents (Fig. 7 *C*). Together, these results suggest that the apparent reduction in unitary amplitude and the fast component of macroscopic current block are controlled by the same Ba^{2+} binding event.

The discrete blocking events observed in single-channel experiments can be subdivided into those events that were present before the channel opened, i.e., closed-blocked channels, and those events that occurred after the channel opened within a given sweep. Blocking events that occurred after the channel opened most likely represent Ba^{2+} block of open channels. However, it is possible that these events occurred during the short closures that can be seen in control records at 30 mV (Fig. 8 *A*). Such blocking events would result from Ba^{2+} block of channels that are closed but very near the open state. In either case, blocking events that occurred after the channel opened would not contribute significantly to the Ba^{2+} block observed in macroscopic currents. The data from macroscopic currents were obtained with a very brief (8 ms) depolarizing command that would have excluded the large majority of these open-blocked or "near open-blocked" events.

Block of closed channels by external Ba^{2+} was evidenced by sweeps that lacked openings during the initial portion of the depolarizing command. In fact, a significant proportion of the sweeps recorded in the presence of 2 mM Ba^{2+} failed to produce even a single opening (Fig. 8 *D*). These blocked times most likely reflect channels that were blocked before the depolarizing command, at which time the channels were closed. These closed-blocked events were quantified as the percentage of sweeps that did not have a single opening during a period equal to three times the mean first latency of 3.4 ± 2.2 ms ($n = 5$), or 10.2 ms. (This duration is similar to the 8-ms depolarizing command used in macroscopic current experiments.) According to this analysis, the likelihood for a channel to open during the first 10.2 ms of a depolarizing command to 30 mV was decreased from 90.2% ± 8.6% ($n = 5$), in control conditions, to 40.6% ± 12.5% ($n = 3$) by 2 mM Ba^{2+}. This suggests that, in the presence of 2 mM Ba^{2+}, there was an ~55% chance for a channel to be blocked at the time of the test pulse. Given the 1-s interpulse interval used in the single-channel experiments, this value is in good agreement with the fraction of slow block produced by 2 mM Ba^{2+} in macroscopic currents (64.7% ± 3.0%, $n = 4$). The relatively short interpulse interval used in the single-channel experiments would be expected to decrease somewhat the fraction of slow block, because this duration is insufficient to fully recover from any relief of block that occurred during the previous 100-ms depolarizing command (see Fig. 4). Therefore, the simplest interpretation is that the slow component of block in the macroscopic currents resulted from channels that never conducted during the brief depolarizing command.

Model of Ba^{2+} Block

The features of external Ba^{2+} block presented here can be reasonably described by a model consisting of two sequential binding sites (Fig. 11). In this model, the fast component of block results from Ba^{2+} occupancy of a more external binding site, called Site 1. From Site 1, Ba^{2+} can either escape to the external solution or move deeper in the pore to Site 2. The binding and unbinding rates at Site 1 are fast due to the small energy barriers ΔG_1 and $\Delta G_1 + \Delta G_2$. Binding at Site 2, on the other hand,

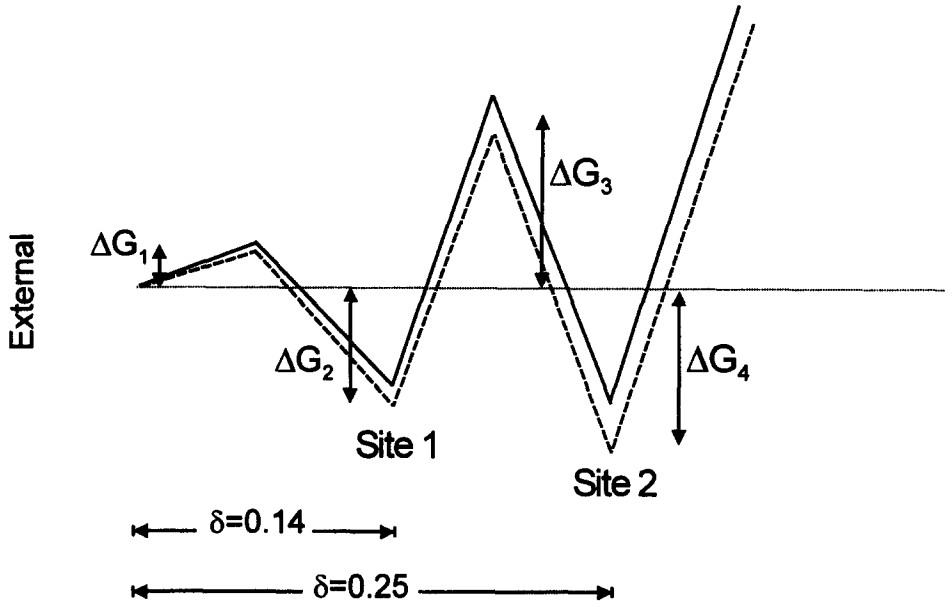

FIGURE 11. Sequential two-site blocking model. Energy profile for a model of two sequential Ba^{2+} binding sites at 0 mV (*continuous line*) and −90 mV (*dashed line*). The energy wells at Site 1 and Site 2 are the two Ba^{2+} binding sites; δ is the fraction of the electric field. The rates of binding and unbinding at Site 1 are fast due to the small energy barriers ΔG_1 and $\Delta G_1 + \Delta G_2$. From Site 1, Ba^{2+} can either return to external solution or move deeper in the pore to Site 2. The binding rate at Site 2 is dependent on both the relatively large energy barrier $\Delta G_2 + \Delta G_3$ and the probability that Site 1 is occupied by Ba^{2+}.

is much slower due to the large energy barrier $\Delta G_2 + \Delta G_3$; this binding event gives rise to the slow component of block in macroscopic currents. Because Ba^{2+} can access Site 2 only from Site 1, the blocking rate at Site 2 is also dependent on the probability that Site 1 is occupied by Ba^{2+}. Consequently, the blocking rate at Site 2 will saturate at high blocker concentrations when Site 1 becomes maximally occupied. This model does not exclude the possibility that both sites can simultaneously be occupied by Ba^{2+}; however, double occupancy may be energetically unfavorable due to ion–ion repulsion (e.g., Newland, Adelman, Tempel, and Almers, 1992). The experiments presented here do not discriminate between single or double occupancy owing to the large difference in affinity between the two sites.

A barium ion residing at Site 2 would exit the channel by moving first to Site 1 and then to the external solution. Because these two sites are in series and the exit from Site 1 is fast compared with the transition from Site 2 to Site 1, this leaving rate should simply reflect the rate limiting transition of Ba^{2+} moving from Site 2 to Site 1. This is consistent with the observed wash-out time course of 20 mM Ba^{2+}, which is slow and composed of only a single component (Fig. 2 *A*). In other words, if these two sites were not in series, or if the fast component was a nonspecific effect of charge screening, the recovery phase should have both a fast and a slow component.

In summary, external Ba^{2+} blocks *Sh*H4-IR at two distinct and sequential sites. Ba^{2+} binding at the external site gives rise to the fast component of block in macroscopic currents. This component results from a very rapid binding and unbinding event that is evidenced in single-channel records as an apparent reduction in unitary amplitude. Once at this external site, Ba^{2+} can move deeper in the pore to a second site; this binding event produces the slow component of block in macroscopic currents. The slow component results from channels that become Ba^{2+} bound before opening, which renders those channels unlikely to conduct during a brief depolarization. The simplest mechanism that can account for this slow component of block is that Ba^{2+} physically occludes K^+ conduction through the pore when it occupies the deeper binding site. However, an additional contributing factor may be that Ba^{2+} occupancy of this deeper site slows the final transition from the closed to open state (Armstrong et al., 1982).

The features of the slow component of block provide information about this deeper Ba^{2+} binding site. For example, the relief of the slow component by internal K^+ suggests that this binding site lies within the channel conduction pathway (Fig. 4; e.g., Bezanilla and Armstrong, 1972). To reach this site, Ba^{2+} crosses ~25% of the membrane electric field (Fig. 3; Woodhull, 1973). Potassium competes with Ba^{2+} at this deeper blocking site, as evidenced by the competition between external K^+ and the slow component of Ba^{2+} block (Fig. 5 *D*). Together, these data present the possibility that the binding site controlling the slow component of Ba^{2+} block is a site used by K^+ in the normal conduction process.

We are grateful to Yuguang Jin for injecting and maintaining *Xenopus* oocytes and to Zhaorong Jiang for preparing mRNA.

This work was supported by grants GM50550 from the National Institutes of Health (E. Stefani and L. Toro) and 94-0227 from Fondo Nacional de Investigaciones, Chile (R. Latorre).

Original version received 24 March 1995 and accepted version received 24 July 1995.

REFERENCES

Adelman, W., and R. J. French. 1978. Blocking of squid axon potassium channel by external caesium ions. *Journal of Physiology.* 276:13–25.

Almers, W. 1978. Gating currents and charge movements in excitable membranes. *Reviews of Physiology, Biochemistry and Pharmacology.* 82:96–190.

Århem, P. 1980. Effects of rubidium, caesium, strontium, barium and lanthanum on ionic currents in myelinated nerve fibers of *Xenopus laevis*. *Acta Physiologica Scandinavica.* 108:7–16.

Armstrong, C. 1966. Time course of TEA^+-induced anomalous rectification squid giant axons. *Journal of General Physiology.* 50:491–503.

Armstrong, C. 1969. Inactivation of the potassium conductance and related phenomena caused by quaternary ammonium ion injected in squid axons. *Journal of General Physiology.* 54:553–575.

Armstrong, C. 1971. Interaction of tetraethylammonium ion derivatives with the potassium channels of giant axons. *Journal of General Physiology.* 58:413–437.

Armstrong, C. M., R. P. Swenson, and S. R. Taylor. 1982. Block of squid axon K channels by internally and externally applied barium ions. *Journal of General Physiology.* 80:663–682.

Armstrong, C. M., and S. R. Taylor. 1980. Interaction of barium ions with potassium channels in squid giant axons. *Biophysical Journal.* 30:473–488.

Bezanilla, F., and C. M. Armstrong. 1972. Negative conductance caused by entry of sodium and cesium ions into the potassium channels of squid axons. *Journal of General Physiology.* 60:588–608.

Bezanilla, F., E. Perozo, and E. Stefani. 1994. Gating of *Shaker* K^+ channels: II. The components of gating currents and a model of channel activation. *Biophysical Journal.* 66:1011–1021.

Coronado, R., and C. Miller. 1979. Voltage-dependent caesium blockade of a cation channel from fragmented sarcoplasmic reticulum. *Nature.* 280:807–810.

Eaton, D. C., and M. S. Brodwick. 1980. Effects of barium on the potassium conductance of squid axon. *Journal of General Physiology.* 75:727–750.

Gaddum, J. H. 1936. The quantitative effects of antagonistic drugs. *Journal of Physiology.* 89:7P.

Grissmer, S., and M. D. Cahalan. 1989. Divalent ion trapping inside potassium channels of human T lymphocytes. *Journal of General Physiology.* 93:609–630.

Hille, B. 1992. Ionic Channels of Excitable Membranes. Sinauer Associates, Sunderland, MA.

Horn, R., J. Patlak, and C. F. Stevens. 1981. The effect of tetramethylammonium on single sodium channel currents. *Biophysical Journal.* 36:321–327.

Hoshi, T., W. N. Zagotta, and R. W. Aldrich. 1990. Biophysical and molecular mechanism of *Shaker* potassium channel inactivation. *Science.* 250:533–538.

Hurst, R. S., L. Toro, and E. Stefani. 1995. External barium block is altered by amino acid substitution at the outer pore of the *Shaker* potassium channel. *Biophysical Journal.* A129. (Abstr.)

Imoto, K., C. Methfessel, B. Sakmann, M. Mishina, Y. Mori, T. Konno, K. Fukuda, M. Kurasaki, H. Bujo, Y. Fujita, and S. Numa. 1986. Location of a δ-subunit region determining transport through the acetylcholine receptor channel. *Nature.* 324:670–674.

Kell, M. J., and L. J. DeFelice. 1988. Surface charge near the cardiac inward-rectifier channel measured from single-channel conductance. *Journal of Membrane Biology.* 102:1–10.

Koren, G., E. R. Liman, D. E. Logothetis, B. Nadal-Ginard, and P. Hess. 1990. Gating mechanisms of a cloned potassium channel expressed in frog oocytes and mammalian cells. *Neuron.* 2:39–51.

Lopez, G. A., Y. N. Jan, and L. Y. Jan. 1994. Evidence that the S6 segment of *Shaker* voltage-gated K^+ channel comprises part of the pore. *Nature.* 367:179–182.

MacKinnon, R., R. Latorre, and C. Miller. 1989. Role of surface electrostatics in the operation of a high-conductance Ca^{2+}-activated K^+ channel. *Biochemistry.* 28:8092–8099.

McCormack, K., W. J. Joiner, and S. H. Heinemann. 1994. A characterization of the activating structural rearrangements in voltage-dependent *Shaker* K^+ channels. *Neuron.* 12:301–315.

Newland, C. F., J. P. Adelman, B. L. Tempel, and W. Almers. 1992. Repulsion between tetraethylammonium ions in cloned voltage-gated potassium channels. *Neuron.* 8:975–982.

Slesinger, P. A., Y. N. Jan, and L. Y. Jan. 1993. The S4-S5 loop contributes to the ion-selective pore of potassium channels. *Neuron.* 11:739–749.

Stefani, E., L. Toro, E. Perozo, and F. Bezanilla. 1994. Gating of *Shaker* K^+ channels I. Ionic and gating currents. *Biophysical Journal.* 66:996–1010.

Taglialatela, M., J. A. Drewe, and A. M. Brown. 1993. Barium blockade of a clonal potassium channel and its regulation by a critical pore residue. *Molecular Pharmacology.* 44:180–190.

Taglialatela, M., G. E. Kirsch, A. M. J. VanDongen, J. A. Drewe, H. A. Hartmann, R. H. Joho, E. Stefani, and A. M. Brown. 1992. Gating currents from a delayed rectifier K^+ channel with altered pore structure and function. *Biophysical Journal.* 62:34–36.

Taglialatela, M., L. Toro, and E. Stefani. 1992. Novel voltage clamp to record small, fast currents from ion channels expressed in *Xenopus* oocytes. *Biophysical Journal.* 61:78–82.

Vergara, C., and R. Latorre. 1983. Kinetics of Ca^{2+}-activated K^+ channels from rabbit muscle incorporated into planar bilayers. *Journal of General Physiology.* 82:543–568.

Wollmuth, L. P. 1994. Mechanism of Ba^{2+} block of M-like K channels of rod photoreceptors of tiger salamanders. *Journal of General Physiology.* 103:45–66.

Woodhull, A. M. 1973. Ionic blockage of sodium channels in nerve. *Journal of General Physiology*. 61: 687–708.

Yellen, G. 1984. Ionic permeation and blockade in Ca^{2+}-activated K^+ channels of bovine chromaffin cells. *Journal of General Physiology*. 84:157–186.

Zagotta, W., and R. W. Aldrich. 1990. Voltage-dependent gating of *Shaker* A-type potassium channels in *Drosophila* muscle. *Journal of General Physiology*. 95:29–60.